

Neutron diffraction and linear Grüneisen parameter studies of magnetism in NdFe₂Ga₈

Xingyu Wang,^{1,2} Cuixiang Wang^{ⓧ, 1,3,2}, Bo Liu,^{1,2} Ke Jia,^{1,2} Xiaoyan Ma,^{1,2} Gang Li,^{1,4} Xiaoping Wang^{ⓧ, 5},
Chin-Wei Wang^{ⓧ, 6}, Youguo Shi,^{1,3,4,*} Yi-feng Yang,^{1,2,4,†} and Shiliang Li^{ⓧ, 1,2,4,‡}

¹Beijing National Laboratory for Condensed Matter Physics, Institute of Physics, Chinese Academy of Sciences, Beijing 100190, China

²School of Physical Sciences, University of Chinese Academy of Sciences, Beijing 100190, China

³Center of Materials Science and Optoelectronics Engineering, University of Chinese Academy of Sciences, Beijing 100049, China

⁴Songshan Lake Materials Laboratory, Dongguan, Guangdong 523808, China

⁵Neutron Scattering Division, Oak Ridge National Laboratory, Oak Ridge, Tennessee 37831, USA

⁶Neutron Group, National Synchrotron Radiation Research Center, Hsinchu 30076, Taiwan



(Received 15 September 2021; revised 16 January 2022; accepted 18 January 2022; published 31 January 2022)

We study the magnetism in NdFe₂Ga₈ by the neutron-diffraction and temperature-modulated linear Grüneisen parameter measurements. Previous thermodynamical measurements have demonstrated that there are two magnetic transitions at 10 and 14.5 K, respectively. Neutron-diffraction measurements confirm that the lower one is an antiferromagnetic (AFM) transition with a commensurate magnetic structure. Both the commensurate and the incommensurate (IC) magnetic peaks are found below the higher transition but their intensities only gradually increase with decreasing temperature. Below 10 K, the commensurate peak intensity increases quickly with decreasing temperature, signaling the AFM transition, while the IC peak intensity disappears below 5 K. The linear Grüneisen parameter along the *c* axis, Γ_c , shows a hysteresis behavior that is different from the hysteresis behavior for the magnetization *M*. We give a discussion of the origin of the magnetism in NdFe₂Ga₈.

DOI: [10.1103/PhysRevB.105.035152](https://doi.org/10.1103/PhysRevB.105.035152)

I. INTRODUCTION

The study of heavy-fermion materials has long been one of the important fields in condensed matter physics. Recently, the so-called 1-2-8 system, i.e., LnM_2T_8 ($Ln = La, Nd, Ce, \text{ etc.}; M = Fe, Co, Ru, \text{ etc.}; T = Al, Ga, In$), has attracted increasing interests [1]. These materials have the CaCo₈Al₈-type structure with the space group of *Pbam* with L_n ions forming one-dimensional (1D) chains along the *c* axis [2]. The magnetic properties are mainly determined by the rare-earth elements as in many other heavy-fermion materials. For example, an antiferromagnetic (AFM) order is found in Pr-based and Eu-based compounds [3–12]. A ferromagnetic order is found in CePd₂Al₈ with $T_c = 9.5$ K, but it has a monoclinic crystal structure [13]. For the Ce-based compounds with the orthorhombic structure, no magnetic ordering is found [14–19]. The CeCo₂Ga₈ is shown to be a rare example of a quasi-1D Kondo chain [17], but its low-temperature properties show 2D quantum critical behaviors including the temperature dependence of the magnetic susceptibility ($\chi \sim T^{-0.2}$), the specific heat ($C/T \sim -\ln T$), and the resistivity ($\rho \sim T^n$ with $n \sim 1$), which may be associated with a quantum critical point [18,19].

The Nd-based 1-2-8 compounds have been relatively less studied. The NdCo₂Al₈ exhibits an AFM order at 8.7 K [9,20]. Interestingly, NdFe₂Ga₈ has two magnetic transitions at about

15 and 10 K [21], which is unique in the 1-2-8 compounds. Both transitions are hardly affected by the magnetic field within the *ab* plane, but they can be quickly suppressed by the field along the *c* axis. At 7 T where magnetic transitions are completely suppressed, the system shows quantum criticality of the conventional 3D spin-density-wave type, such as $\rho \sim T^{1.5}$ and $C/T \sim T^{-0.5}$. While both transitions have been assumed to be AFM in nature, the magnetic structures have not been identified. Moreover, a hysteresis behavior is found in the magnetic-susceptibility and resistivity measurements, and its origin is still unknown.

In this work, we studied the magnetic structure of NdFe₂Ga₈ by the neutron-diffraction technique. We found that the transition at $T_N \sim 10$ K is from a long-range commensurate AFM order. Below the higher transition temperature $T_O \sim 14.5$ K, both incommensurate (IC) and commensurate magnetic peaks gradually appear. The intensities of the IC peaks become maximum at T_N and decrease to zero at about 5 K. The field dependence of the linear Grüneisen parameter along the *c* axis, Γ_c , shows several maximums and a hysteresis behavior that is different from that of the magnetization *M*. Our results suggest that the magnetic orders are complicated.

II. EXPERIMENTS

Single crystals of NdFe₂Ga₈ were grown by the self-flux method as reported previously [21]. Neutron single-crystal diffraction (NSCD) measurement was carried out on a 113-mg single-crystal sample on the TOPAZ diffractometer at the Spallation Neutron Source, Oak Ridge National Laboratory. Five grams of single crystals were ground to powders

*ygshi@iphy.ac.cn

†yifeng@iphy.ac.cn

‡slli@iphy.ac.cn

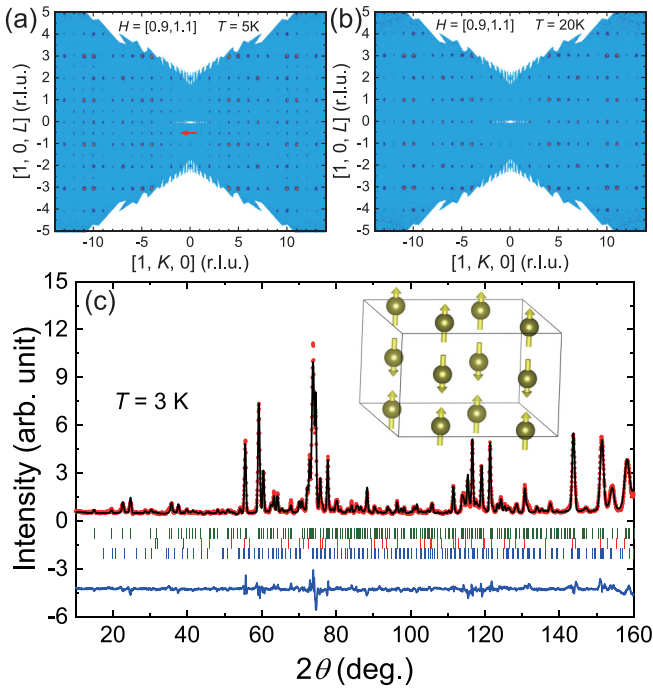


FIG. 1. (a) and (b) NSCD patterns in the $(1, K, L)$ plane at 5 and 20 K, respectively. The brackets for H give the integrated range along the H direction. The arrow in (a) indicates a new peak appeared at half integer L . (c) NPD intensity at 3 K. The calculated intensities are shown by the black line. Short vertical green and blue lines represent calculated nuclear and magnetic Bragg peak positions, respectively. Vertical red lines represent peaks from FeGa_3 impurities. The blue line shows the difference between measured and calculated intensities. The weighted profile R factor (R_{wp}) is 10.2. The inset shows the magnetic structure with the moments sitting on Nd sites.

and measured by the neutron powder diffraction (NPD) on the Echidna diffractometer at the Australian Nuclear Science and Technology Organization. The refinements for the NSCD and NPD data were done by using the Jana and Fullprof programs, respectively [22,23]. The linear Grüneisen parameter was measured by a homemade temperature-modulated dilatometer [24] putting in a physical property measurement system (Quantum Design) and a 18-T magnet with a top-loading ^3He fridge. The dimension of the sample is about 0.2 mm in diameter and 4 mm in length. The sample was attached on the top of the piezobender and CuBe frame by glue and self-heated by two silver-paint contacts. Several heating currents have been tested to make sure that the measurement is in the optimal condition [24].

III. RESULTS AND DISCUSSIONS

Figures 1(a) and 1(b) show the NSCD patterns of NdFe_2Ga_8 in the $[1, K, L]$ plane at 5 and 20 K, respectively. Compared with 20-K data, new peaks appear at 5 K at half integer L , suggesting the appearance of long-range AFM order. Nuclear structure was refined at 20 K with 23033 peaks and the result is the same as previously reported [21]. At 5 K, no change of nuclear structure is found and the magnetic structure is refined by the 5231 magnetic peaks with a total

wR of 26.36. Figure 1(c) shows the NPD data at 3 K and the refinement for both nuclear and magnetic structures gives the magnetic R factor as 60.5. About 3.2% of FeGa_3 impurity is found in the NPD pattern. We note that this impurity does not affect the NSCD refinement as it has the form of polycrystalline and its diffraction intensity in the single-crystal sample is thus very weak. In both refinements, the magnetic form factor has included both $\langle j_0 \rangle$ and $\langle j_2 \rangle$ terms. Both the single-crystal and the polycrystalline refinements give the same magnetic structure as shown in the inset of Fig. 1(c). The magnetic moments point to the c axis and are aligned ferromagnetically within the ab plane but antiferromagnetically along the c axis. The value of the ordered moment from the NSCD and NPD is $3.379 \pm 0.016 \mu_B$ at 5 K and $3.31 \pm 0.15 \mu_B$ at 3 K, respectively.

We note that the above refinements have assumed that the moments are on the Nd sites. If the moments are added on Fe sites, the value on Fe1 site is negligible, while that on the Fe2 site is about $0.593(29)$ and $0.544(27) \mu_B$ for Fe^{2+} and Fe^{3+} magnetic form factors used in refinements, respectively, which are much smaller than the moments on Nd sites. However, we find no improvement to the fit with the Fe moments included and the Nd moments are almost the same as before. Therefore we conclude that Nd^{3+} is the only magnetic ion in the magnetic ordering of NdFe_2Ga_8 . A similar conclusion has also been found in PrFe_2Al_8 [5].

Figures 2(a) and 2(b) show the magnetic Bragg peaks at $(1, 4, -0.5)$ cutting along the H and K directions, respectively. With the peak intensity decreasing with increasing temperature, the peak can always be well fitted by the Gaussian function with no change of the width. For the cuts along the L direction [Fig. 2(c)], while the peak can still be fitted by the Gaussian function at low temperatures, two new peaks emerge at the IC positions ($L \sim -0.5 \pm \delta$) with $\delta \approx 0.05$ at high temperatures. A three-Gaussian function with the sum of three individual Gaussian functions is thus introduced to fit the data, as shown in Fig. 2(d). Since we are unable to refine the magnetic structure for the IC peaks, it is not known whether Fe may play a role in this phase or not.

Figure 2(e) shows the colormap for the intensity as a function of L and temperature. The incommensurability δ varies little above 10 K and seems to decrease with decreasing temperature below 10 K. The full width at half maximums for the commensurate and IC peaks are both temperature independent and comparable to the instrumental resolution, indicating that both of the peaks are associated with long-range orders.

Figure 2(f) shows the temperature dependence of the peak intensities at the commensurate and IC positions. Below 10 K, the commensurate one can be fitted by the function $I_0(1 - T/T_N)^{2\beta}$ with T_N fixed 10 K. The fitted β is 0.31 ± 0.03 . The IC peak intensity shows totally different behaviors. Above T_N , the temperature dependence of both commensurate and IC peak intensities is the same. Within our resolution, we can only identify the appearance of magnetic peaks at 13 K. With decreasing temperature, the IC peak intensity reaches a maximum at T_N and decreases with further cooling temperature, whereas the commensurate peak intensity quickly increases as a regular AFM transition. The IC peaks completely disappear below $T^* \approx 5$ K. This suggests that the IC phase may compete with the low-temperature commensurate magnetic phase.

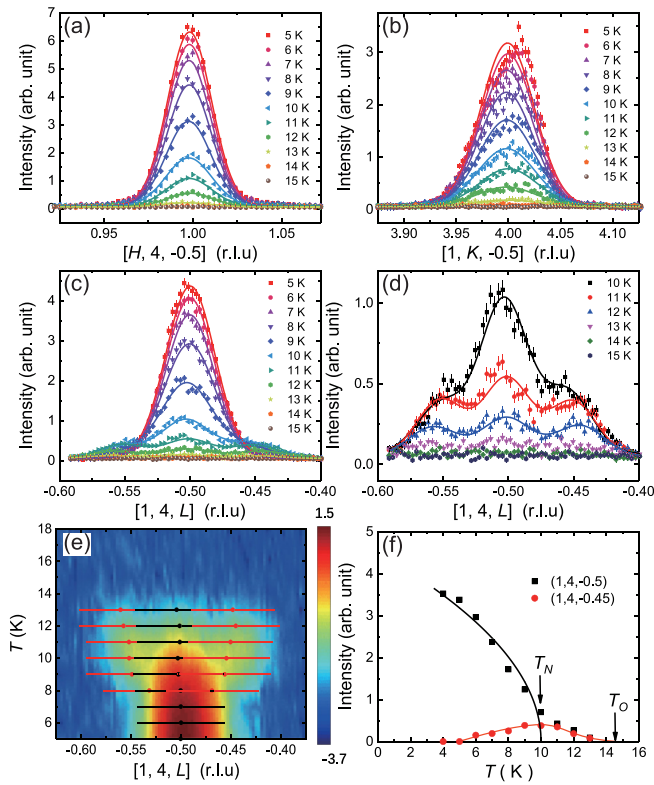


FIG. 2. (a) and (b) The cuts at $(1, 4, -0.5)$ peak from the NSCD data at different temperatures along the H and K directions, respectively. The solid lines are fitted by the Gaussian function. (c) The cuts at $(1, 4, -0.5)$ peak along the L direction at different temperatures. The solid lines are fitted by the three-Gaussian function. Panel (d) shows the data in (c) for temperatures from 10 to 15 K. (e) The colormap for the intensity at $(1, 4, -0.5)$ in logarithmic scale. The dots mark the centers of the commensurate and IC peaks. The horizontal bars give the FWHMs of the peaks. (f) The temperature dependence of the peak intensity at $(1, 4, -0.5)$ and $(1, 4, -0.45)$. The black solid line is fitted by the function as described in the text. The red line is a guide to the eye.

To further investigate the nature of the magnetic transitions in NdFe_2Ga_8 , we studied the linear Grüneisen parameter Γ_c , where the linear thermal expansion is measured along the c axis [24]. Figure 3(a) shows the temperature dependence of Γ_c in the field-cooling (FC) process, which is small and positive at high temperatures for all fields. At zero field, Γ_c changes to negative with decreasing temperature and its absolute value quickly increases until $T = T_O$. With a kink at T_O , $|\Gamma_c|$ continues to increase with decreasing temperature and shows another kink at T_N . Below T_N , $|\Gamma_c|$ initially changes little with decreasing temperature and then quickly decreases with decreasing temperature below T^* . With field increasing, T_O decreases and seems to merge together with T_N above 3 T, which is consistent with previous reports [21]. The round feature associated with T^* decreases with the increasing field and cannot be seen above 3 T. Further increasing the field makes it hard to identify T_N and T_O , while $|\Gamma_c|$ at 1.8 K becomes maximum at 5 T and starts decreasing with increasing field. Interestingly, Γ_c at low temperature changes continuously

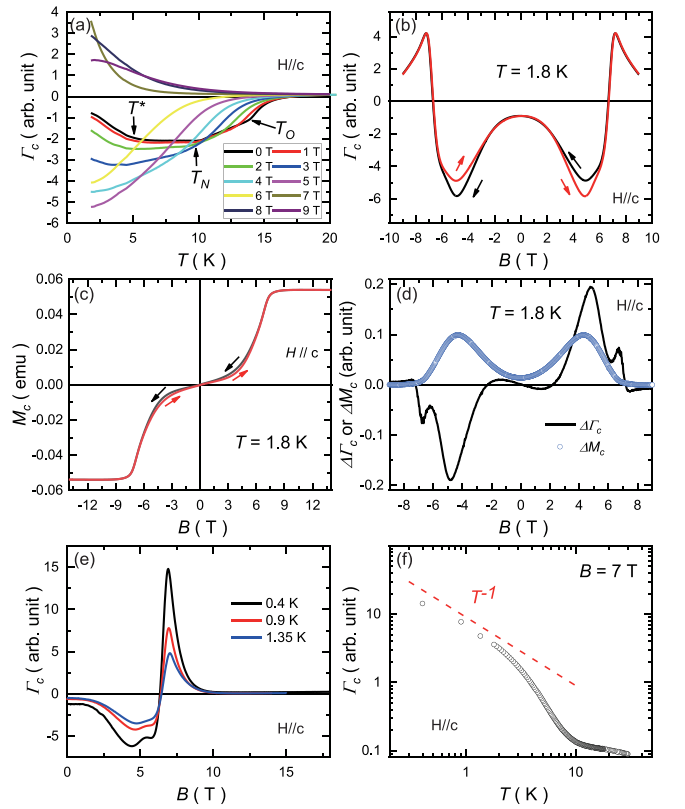


FIG. 3. (a) Temperature dependence of the linear Grüneisen parameter Γ_c at various fields. The measurements were made in the FC process. The arrows indicate T_O and T_N at zero field. (b) Field dependence of Γ_c at 1.8 K. The arrows indicate the field-decreasing and field-increasing processes. (c) Field dependence of M_c at 1.8 K. The arrows indicate the field-decreasing and field-increasing processes. (d) Field dependence of $\Delta\Gamma_c$ and ΔM_c at 1.8 K. (e) Field dependence of Γ_c below 1.8 K for a different sample. The measurements were made with the field-decreasing process. (f) Γ_c as a function of temperature at 7 T in the log-log scale. The values below 1.8 K are taken from the data in (e) and normalized to those above 1.8 K. The dashed line represents the T^{-1} dependence.

from negative to positive value when the field increases from 6 to 7 T.

Figure 3(b) shows the field dependence of Γ_c at 1.8 K, where the positive and negative maximums appear at about 7 and 5 T, respectively. Figure 3(c) shows the field dependence of M_c with the field parallel to c at 1.8 K. M_c becomes fully saturated above about 9 T. Hysteresis behaviors are found between increasing and decreasing field processes for both measurements. Figure 3(d) further shows the field dependence of $\Delta\Gamma_c = \Gamma_c^{dec} - \Gamma_c^{inc}$, which is the difference of Γ_c between the decreasing and the increasing field processes. As a comparison, the field dependence of $\Delta M_c = M_c^{dec} - M_c^{inc}$ is also shown. Surprisingly, there are two maximums in $\Delta\Gamma_c$ at about 4.8 and 6.8 T, but only one maximum exists in ΔM_c at about 4.3 T. Moreover, the value of $\Delta\Gamma_c$ is initially small and changes sign at about 2.2 T. Its value increases dramatically above 3 T, while ΔM_c smoothly increases with increasing field until it reaches its maximum at 4.3 T. These

results suggest that the hysteresis behaviors in Γ_c and M_c have different origins.

Figure 3(e) shows Γ_c in the field-decreasing process down to 0.4 K. Interestingly, two-peak features appear around 5 T at 0.4 K, which indicates complicated behaviors within the ordering state. We note that the transitions at T_O and T_N behave very differently in the field in that the former is easily suppressed by the field whereas the latter is little affected by the field below 3 T where the two transitions merge together [21]. The features around 5 T may thus be related to the couplings between the orders associated with T_O and T_N . Nevertheless, here we are more interested in the properties around 7 T, which has been shown to exhibit quantum criticality [21]. Figure 3(f) shows the temperature dependence of Γ_c at 7 T, which exhibits a divergent behavior with $\Gamma_c \propto T^{-1}$ below 2 K.

With the results above, we can get a more comprehensive understanding on the magnetic orderings in NdFe₂Ga₈. The magnetic transition at $T_N \sim 10$ K is clearly associated with the commensurate AFM structure. Between T_N and T_O , one commensurate and two IC peaks are observed. The IC magnetic structure may be explained as a SDW order [21]. This IC magnetism seems to compete with the commensurate order as the intensities of the IC peaks gradually decrease with decreasing temperature below T_N and finally become zero below T^* [Fig. 2(f)]. This competition seems to also present under field as T^* is suppressed under field [Fig. 3(a)], which suggests that the IC peaks may be evoked by the magnetic field.

There are some interesting features that need to be further discussed. First, the emergence of the IC peaks below T_O does not look like the temperature dependence of a typical order parameter while the specific-heat jump at T_O clearly indicates that the transition is a second-order transition. By forcing a fit of $I_0(1 - T/T_O)^{2\beta}$ for the IC peak intensity above T_N , we get a value of β much larger than 0.5, which is hard to understand. Second, $\Delta\Gamma_c$ shows two peaks whereas ΔM_c shows just one, as shown in Fig. 3(d). The high-field peak of $\Delta\Gamma_c$ is located at the field around which Γ_c changes quickly from negative value to positive value, which is typically associated with a dramatic change of the electronic state. This peak cannot be found in ΔM_c , suggesting that it is not related to the dipole moments. As discussed above, the competition between the commensurate and IC magnetism may present under magnetic field, but it cannot completely explain the hysteresis in $M - H$ and $\Gamma_c - H$ since they have different behaviors.

The above results suggest that the magnetic phase below T_O may not be a conventional SDW as expected previously [21].

One possibility is that the system is close to a Lifshitz point [25] where the AFM and modulated phases could coexist, but whether this scenario can explain the above results is not known. We propose another possibility that the IC phase may be a MO [26,27], which gives a natural explanation on why the temperature dependence of the IC peaks does not look like an order parameter. In this case, the hysteresis of Γ_c is determined by the field dependence of MO or its competition with the long-range AFM order. We note that a MO could in principle result in large magnetic anisotropy and IC magnetic peaks. If a MO indeed exists in NdFe₂Ga₈, the itinerancy of electrons should play a major role as shown by the behaviors of the resistivity and linear Grüneisen parameter. Of course, there is still a lack of direct evidence for the existence of a MO and further studies on this system are needed.

IV. CONCLUSIONS

In conclusion, we have found both commensurate and IC magnetic peaks in the magnetic ordered states of NdFe₂Ga₈. While the low-temperature commensurate peaks are associated with the AFM transition at 10 K, the IC peaks cannot be simply understood within the picture of a conventional SDW. The measurements on the linear Grüneisen parameter suggests that its behaviors may not be related to the dipole moments. While there are possibilities that theories based on the dipole moments may explain this, we suggest that a MO with strong itinerant characteristics could provide a simple answer.

ACKNOWLEDGMENTS

This work is supported by the National Key R&D Program of China (Grants No. 2020YFA0406003, No. 2017YFA0302900, No. 2017YFA0303100, No. 2016YFA0300502, and No. 2016YFA0300604), the National Natural Science Foundation of China (Grants No. 11874401, No. 11674406, No. 11961160699, No. 11774399, and No. U2032204), the Strategic Priority Research Program of the Chinese Academy of Sciences (Grant No. XDB33010000), the Beijing Natural Science Foundation (Z180008), and the K.C. Wong Education Foundation (GJTD-2020-01, GJTD-2018-01). The single-crystal neutron diffraction experiment on TOPAZ used resources at the Spallation Neutron Source, a DOE Office of Science User Facility operated by the Oak Ridge National Laboratory, USA.

- [1] M. O. Ogunbunmi, Electronic and magnetic properties of the quasi-skutterudite RT₂X₈ intermetallic compounds, *Prog. Solid State Ch.* **58**, 100275 (2020).
- [2] O. M. Sichevich, R. V. Lapunova, Y. N. Grin, and Y. P. Yarmolyuk, Intermetallic compounds RGe₈Fe₂ and RGe₈Co₂ (R= La, Ce, Pr, Nd, Sm, Eu), *Izvestiya Akademii Nauk SSSR, Metall* **6**, 117 (1985).
- [3] O. Tougaard, D. Kaczorowski, and H. Noël, PrCo₂Al₈ and Pr₂Co₆Al₁₉: Crystal structure and electronic properties, *J. Solid State Chem.* **178**, 3639 (2005).

- [4] H. S. Nair, S. K. Ghosh, K. R. Kumar, and A. M. Strydom, Magnetic ordering and crystal field effects in quasi-caged structure compound PrFe₂Al₈, *J. Phys. Chem. Solids* **91**, 69 (2016).
- [5] H. S. Nair, M. O. Ogunbunmi, C. M. N. Kumar, D. T. Adroja, P. Manuel, D. Fortes, J. Taylor, and A. M. Strydom, Pr-magnetism in the quasi-skutterudite compound PrFe₂Al₈, *J. Phys.: Condens. Matter* **29**, 345801 (2017).
- [6] M. O. Ogunbunmi, H. S. Nair, and A. M. Strydom, Superzone gap formation and possible kondo-like features in the heavy

- fermion PrFe_2Ga_8 compound, *JPS Conf. Proc.* **30**, 011114 (2020).
- [7] M. O. Ogunbunmi and A. M. Strydom, Investigation of the magnetic ground state of PrRu_2Ga_8 compound, in *the Proceedings of SAIP2017, the 62nd Annual Conference of the South African Institute of Physics* (The South African Institute of Physics, Lynnwood Ridge, South Africa, 2017), p. 107.
- [8] M. O. Ogunbunmi, B. M. Sondezi, H. S. Nair, and A. M. Strydom, Electronic and magnetic properties of quasi-skutterudite PrCo_2Ga_8 compound, *Phys. B: Condens. Matter* **536**, 128 (2018).
- [9] P. Watkins-Curry, J. V. Burnett, T. Samanta, D. P. Young, S. Stadler, and J. Y. Chan, Strategic crystal growth and physical properties of single-crystalline LnCo_2Al_8 ($\text{Ln} = \text{La-Nd, Sm, Yb}$), *Cryst. Growth Des.* **15**, 3293 (2015).
- [10] V. Fritsch, S. Bobev, N. O. Moreno, Z. Fisk, J. D. Thompson, and J. L. Sarrao, Antiferromagnetic order in $\text{EuRh}_2(\text{Ga, In})_8$, *Phys. Rev. B* **70**, 052410 (2004).
- [11] O. Sichevych, M. Kohout, W. Schnelle, H. Borrmann, R. Cardoso-Gil, M. Schmidt, U. Burkhardt, and Y. Grin, EuTM_2Ga_8 ($\text{TM} = \text{Co, Rh, Ir}$)—A contribution to the chemistry of the CeFe_2Al_8 -type compounds, *Inorg. Chem.* **48**, 6261 (2009).
- [12] N. P. Calta, S. L. Bud'ko, A. P. Rodriguez, F. Han, D. Y. Chung, and M. G. Kanatzidis, Synthesis, structure, and complex magnetism of MIr_2In_8 ($\text{M} = \text{Eu, Sr}$), *Inorg. Chem.* **55**, 3128 (2016).
- [13] A. Tursina, E. Khamitcaeva, D. Gnida, and D. Kaczorowski, CePd_2Al_8 - A ferromagnetic Kondo lattice with new type of crystal structure, *J. Alloys Compd.* **731**, 229 (2018).
- [14] M. Kolenda, M. D. Koterlin, M. Hofmann, B. Penc, A. Szytula, A. Zygmunt, and J. Żukrowski, Low temperature neutron diffraction study of the CeFe_2Al_8 compound, *J. Alloys Compd.* **327**, 21 (2001).
- [15] M. Schlüter and W. Jeitschko, Ternary lanthanoid ruthenium gallides with a high gallium content: $\text{Ln}_2\text{Ru}_3\text{Ga}_{10}$ ($\text{Ln} = \text{Yb, Lu}$) with a new structure type and LnRu_2Ga_8 ($\text{Ln} = \text{La-Nd}$) with CaCo_2Al_8 -type structure, *Inorg. Chem.* **40**, 6362 (2001).
- [16] S. Ghosh and A. M. Strydom, Strongly correlated electron behaviour in CeT_2Al_8 ($\text{T} = \text{Fe, Co}$), *Acta. Phys. Pol. A* **121**, 1082 (2012).
- [17] K. Cheng, L. Wang, Y. Xu, F. Yang, H. Zhu, J. Ke, X. Lu, Z. Xia, J. Wang, Y. Shi, Y. Yang, and Y. Luo, Realization of kondo chain in CeCo_2Ga_8 , *Phys. Rev. Mater.* **3**, 021402(R) (2019).
- [18] L. Wang, Z. Fu, J. Sun, M. Liu, W. Yi, C. Yi, Y. Luo, Y. Dai, G. Liu, Y. Matsushita, K. Yamaura, L. Lu, J.-G. Cheng, Y. feng Yang, Y. Shi, and J. Luo, Heavy fermion behavior in the quasi-one-dimensional Kondo lattice CeCo_2Ga_8 , *npj Quant Mater* **2**, 36 (2017).
- [19] A. Bhattacharyya, D. T. Adroja, J. S. Lord, L. Wang, Y. Shi, K. Panda, H. Luo, and A. M. Strydom, Quantum fluctuations in the quasi-one-dimensional non-fermi liquid system CeCo_2Ga_8 investigated using μSR , *Phys. Rev. B* **101**, 214437 (2020).
- [20] W. He, H. Zhong, H. Liu, J. Zhang, and L. Zeng, Crystal structure and electrical resistivity of NdCo_2Al_8 , *J. Alloys Compd.* **467**, 6 (2009).
- [21] C. Wang, X. Wang, L. Wang, M. Yang, Y. Song, Z. Mi, G. Li, Y. Shi, S. Li, and Y.-f. Yang, Quantum criticality in NdFe_2ga_8 under magnetic field, *Phys. Rev. B* **103**, 035107 (2021).
- [22] V. Petricek, M. Dusek, and L. Palatinus, Crystallographic computing system JANA2006: General features, *Z. Kristallogr.* **229**, 345 (2014).
- [23] J. Rodríguez-Carvajal, Recent advances in magnetic structure determination by neutron powder diffraction, *Physica B.* **192**, 55 (1993).
- [24] Y. Gu, B. Liu, W. Hong, Z. Liu, W. Zhang, X. Ma, and S. Li, A temperature-modulated dilatometer by using a piezobender-based device, *Rev. Sci. Instrum.* **91**, 123901 (2020).
- [25] R. M. Hornreich, The Lifshitz point: Phase diagrams and critical behavior, *J. Mag. Mag. Mater.* **15-18**, 387 (1980).
- [26] P. Santini, S. Carretta, G. Amoretti, R. Caciuffo, N. Magnani, and G. H. Lander, Multipolar interactions in f -electron systems: The paradigm of actinide dioxides, *Rev. Mod. Phys.* **81**, 807 (2009).
- [27] M.-T. Suzuki, H. Ikeda, and P. M. Oppeneer, First-principles theory of magnetic multipoles in condensed matter systems, *J. Phys. Soc. Jpn.* **87**, 041008 (2018).